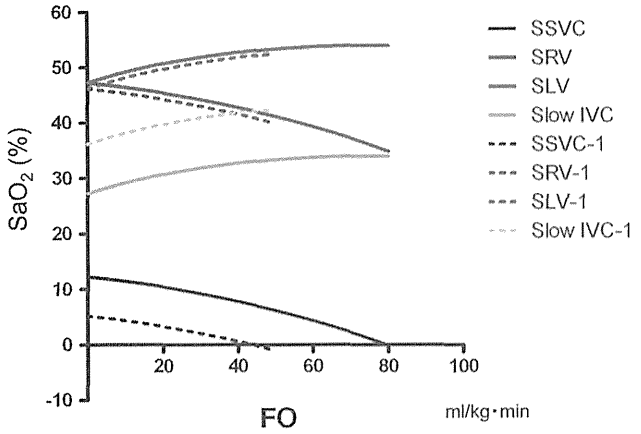

Fig. 2 Relation between the blood flow rate through the foramen ovale and oxygen saturation in the TGA model. *Dashed lines* indicates the results for oxygen saturation at each site in association with the blood flow rate at the foramen ovale (a). *Solid lines* indicate the changes at each site in association with the blood flow rate at the foramen ovale (a)

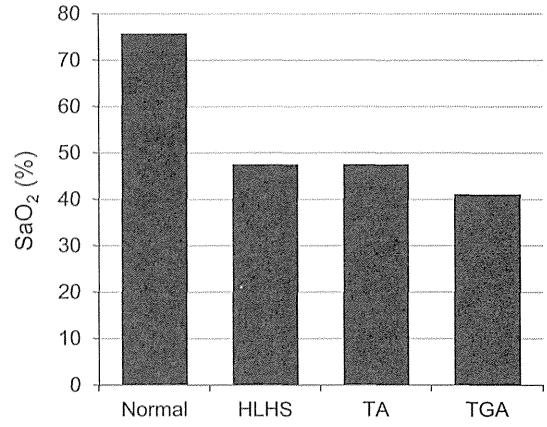

Fig. 3 Results of cerebral oxygen saturation for each CHD model

to those in the normal circulation, and oxygen saturation in the upper and lower limbs in TGA was equal to $S_{RV}O_2$ and $S_{LV}O_2$, respectively:

$$S_{RV}O_2 - S_{SVC}O_2 = 41\,\%$$

$$S_{LV}O_2 - S_{low\,IVC}O_2 = 10\,\%.$$

Furthermore, the equation used for oxygen saturation of blood mixed in the right ventricle was

$$S_{RV}O_2 = ([80 \times S_{low\,IVC}] + [(200 - a) \times 85\,\%] + [170 \times S_{SVC}])/(450 - a).$$

The equation used for oxygen saturation of blood mixed in the left ventricle was

$$S_{LV}O_2 = ([130 \times S_{LV}] + [a \times 85\,\%])/(130 + a) \qquad (*)$$

On the basis of these equations, the following equation was derived:

$$S_{SVC}O_2 = ([44 \times a^2] + [1,170 \times a] - 133,900)/([a^2 - 150] \times [a - 26,000]).$$

Subsequently, oxygen saturation was calculated as follows:

$$S_{RV}O_2 = S_{SVC} + 41$$

$$S_{LV}O_2 = (*)$$

$$S_{low\,IVC}O_2 = S_{LV} - 10$$

Figure 2 (dashed lines) shows the results for oxygen saturation at each site in association with the blood flow rate at the foramen ovale (a).

Reexamination of the Hypothesis of TGA

When the blood flow rate at the foramen ovale was $a = 0$, the $S_{SVC}O_2$ obtained in "Reexamination of the hypothesis of TA" section was the highest at 5.15 %, a value that was too low physiologically. While the hypothesis that blood flow rates and oxygen consumption in both the upper and the lower limbs were similar to those in the normal circulation was maintained, the simulation of the normal circulation was changed as in "Reexamination of the hypothesis of HLHS" section. Furthermore, because the blood flow rate in the lower limbs was estimated to be low owing to high pulmonary blood flow in TGA, the decrease in oxygen saturation in the lower limbs was estimated to be slightly higher, in accordance with the following hypotheses:

$$S_{RV}O_2 - S_{SVC}O_2 = 30\,\%$$

$$S_{LV}O_2 - S_{low\,IVC}O_2 = 25\,\%$$

Furthermore, as with the previous simulation, the equation used for the oxygen saturation of blood mixed in the right ventricle was

$$S_{RV}O_2 = ([80 \times S_{low\,IVC}] + [(200 - a) \times 85\,\%] + [170 \times S_{SVC}])/(450 - a).$$

The equation used for the oxygen saturation of blood mixed in the left ventricle was

$$S_{LV}O_2 = ([130 \times S_{LV}] + [a \times 85\,\%])/(130 + a) \qquad (*)$$

On the basis of these equations, the following equation was derived:

$$S_{SVC}O_2 = ([50 \times a^2] + [50 \times a] - 318,500)/([a^2 - 150] \times [a - 26,000]).$$

Subsequently, oxygen saturation was calculated as follows:

$$S_{RV}O_2 = S_{SVC} + 30$$

$$S_{LV}O_2 = (*)$$

$$S_{low\,IVC}O_2 = S_{LV} - 25$$

Figure 2 (solid lines) shows the changes at each site in association with the blood flow rate at the foramen ovale (*a*).

When the blood flow rate at the foramen ovale (*a*) was hypothesized to be 130 mL kg^{-1} min^{-1} as in the normal circulation, this simulation yielded $S_{SVC} = 13.3$ %, $S_{low\ IVC} = 20.7$ %, $S_{LV} = 45.7$ %, and $S_{RV} = 43.2$ %, which were lower than those obtained from the HLHS and TA simulations.

The results of cerebral oxygen saturation for each site in CHDs are summarized in Fig. 3.

Discussion

Although in recent years, ≥90 % of CHD patients have been saved owing to improved surgical outcomes, it has been widely recognized that there are many patients who develop various postoperative neuropsychiatric developmental abnormalities (affecting motor function, language, visuospatial perception, behavior, and learning) [11, 14]. Although the causes of these abnormalities may be multifactorial, the involvement of brain injury in utero is suggested by reports on decreased head circumference at birth [1, 10], delayed myelination detected by preoperative magnetic resonance imaging of newborns [9], and abnormal fetal cerebral blood flow waveforms demonstrated using the Doppler ultrasound [4, 5, 15]. Most notably, structural anomalies in CHD may be closely associated with decreased volume and oxygen saturation of cerebral blood flow, and abnormalities in oxygen supply to the brain may play a role in brain injury in utero. To address these issues, we performed a simulation study to obtain theoretical values of the oxygen saturation of cerebral blood flow using a mathematical model of fetal circulation, which allowed us to purely assess the effects of hemodynamic factors due to cardiovascular structural anomalies by eliminating potential confounding factors affecting the cerebral circulation.

Our mathematical model was based on the foundational study by Rudolph et al. [17–19]. By using the microsphere technique, those authors provided, for the first time, data for quantitative blood flow distribution in the fetus in utero. They found an important concept of preferential blood flow streaming to protect fetal cerebral circulation: well-oxygenated blood with an oxygen saturation of 85 % from the placenta passes through the ductus venosus and foramen ovale, and enters into the left ventricle, whereas blood from the SVC with a low oxygen saturation of about 35 % exclusively enters into the right ventricle. By using the information from the experiment of Rudolph's group, in the present study we constructed a model of fetal circulation with HLHS and contrasted it to other forms of CHD that may affect the fetal cerebral circulation. We found that the oxygen saturation of cerebral blood flow in a fetus with HLHS was markedly lower than that of a normal fetus; however, importantly, it was equally low as in a fetus with TA. Furthermore, cerebral oxygen saturation in TGA was even lower than that in HLHS. Although our model did not directly address changes in cerebral blood flow, it provided the oxygen content in blood with the condition of the blood flow being kept equal among the models. Thus, our model should help deduce the potential abnormality in blood flow as discussed below.

Kaltman et al. [8] divided CHD fetuses into those with pulmonary atresia/stenosis or a right-sided obstructive lesion and those with aortic atresia/stenosis including HLHS or a left-sided obstructive lesion, to examine differences in the Doppler patterns of cerebral blood flow using the pulsatility index and the resistance index. They reported that cerebrovascular resistance in the fetuses with a left-sided obstructive lesion was lower than that in the fetuses with a right-sided obstructive lesion, whereas cerebrovascular resistance in the latter fetuses was higher than the normal. Furthermore, decreased head circumference at birth, which is closely associated with neuropsychiatric developmental prognosis, is reported in HLHS at a remarkably higher frequency, as compared with TA [3]. Taking together these results with our present results showing the oxygen saturation of cerebral blood flow in TA (right-sided obstructive lesion) and HLHS to be equal, it is very likely that decreased blood flow or increased oxygen consumption in the brain is already present during the fetal period in HLHS. Because oxygen consumption in the brains of HLHS patients is unlikely to be markedly increased in comparison with that in the brains of TA patients, it is assumed that decreased cerebral blood flow is probably due to hemodynamics specific to HLHS, greatly affecting the cranial nerve development during the fetal period.

Decreased cerebral blood flow in HLHS fetuses is also suggested by a comparison between TGA and HLHS. While decreases in cerebrovascular resistance [7, 22] and head size at birth [4] in TGA fetuses have been reported by several investigators, many reports have shown that the decreases in TGA fetuses are smaller than those in HLHS fetuses. For example, Rosenthal reported that, although head circumference at birth is decreased in relation to body weight in both TGA and HLHS, the decrease is more

pronounced in HLHS [16]. Furthermore, Manzar et al., who directly compared head circumferences at birth adjusted for gestational age between TGA and HLHS, reported that, although the adjusted values were smaller in both TGA and HLHS than the normal value, the difference between the adjusted and normal values was significantly larger in HLHS [13]. These results, together with our present results showing that oxygen saturation of cerebral blood flow in TGA is lower than that in HLHS, strongly suggest that the cerebral blood flow rate is more highly decreased in HLHS than in TGA, as shown by the comparison with TA.

Broadly, there are two possible causes for the decreased cerebral blood flow in HLHS: one is retrograde cerebral perfusion from a patent ductus arteriosus (PDA), which is a characteristic of HLHS, and the other is that the right ventricle, which is the systemic ventricle in HLHS, cannot maintain adequate cardiac output. In this regard, Shillingford et al. reported the important observation that microcephaly in newborns with HLHS was associated with a small ascending aorta, but not a small transverse aortic arch, suggesting the importance of forward flow from the left ventricle for cerebral perfusion [21]. This notion was also supported by a report from Berg et al., who demonstrated that HLHS fetuses with aortic atresia have decreased cerebrovascular impedance and smaller heads, whereas fetuses with severe aortic stenosis and reversal of flow in the aortic arch do not [3]. Kaltman et al. also reported that a decrease in cerebrovascular resistance was more pronounced in HLHS, in which the cerebral blood flow is maintained only by reversal of flow from the arterial duct, than other left-sided obstructive lesions that have antegrade flow from the left ventricle [8]. When these results are considered together, we can reasonably assume, as the main cause, that the cerebral blood flow rate itself in HLHS fetuses is decreased by retrograde cerebral perfusion through a PDA. This is also supported by our recent report showing that cerebral blood flow after bilateral pulmonary artery banding in HLHS patients is more impaired than that after the Norwood procedure [20].

Because cerebrovascular insufficiency also means coronary vascular insufficiency, especially in HLHS patients with aortic atresia, cerebral perfusion is also considered to be possibly impaired by the synergistic effect of right ventricular dysfunction caused by coronary hypoperfusion. This condition results in insufficient uptake of oxygen and nutrients from the placenta and also adversely affects fetal development, which may lead to a vicious cycle resulting in developmental disorders of the brain. In fact, Berg et al. [3], who compared TGA and HLHS fetuses and observed decreased cerebrovascular resistance only in the latter, reported that, when fetuses with growth restriction and uteroplacental dysfunction were excluded, children born with HLHS had only slightly smaller head circumferences than controls, whereas the difference was more pronounced in newborns with TGA. This suggests that abnormalities of not only cerebral blood flow but also those of systemic perfusion may additively and synergistically be involved in developmental disorders of the brain in HLHS.

Conclusion

In this study, we performed simulations to assess the actual differences in the oxygen saturation of cerebral blood flow due to structural anomalies in CHD while excluding other factors that might affect the fetal cerebral circulation. We found the cerebral blood flow rate to be decreased in HLHS, and the main cause was strongly suggested to be retrograde cerebral perfusion through a PDA. These results provide important information about the neurodevelopmental prognosis in HLHS fetuses and simultaneously suggest the need to identify strategies to resolve this unfavorable cerebral circulatory state in utero. Also, future studies linking a mathematical simulation with more sophisticated blood flow modeling with fetal magnetic resonance imaging are needed to further improve our understanding and management of fetal circulation with CHD.

References

1. Barbu D, Mert I, Kruger M, Bahado-Singh RO (2009) Evidence of fetal central nervous system injury in isolated congenital heart defects: microcephaly at birth. Am J Obstet Gynecol 201(43):e1–e7
2. Bellinger DC, Jonas RA, Rappaport LA, Wypij D, Wernovsky G, Kuban KC, Barnes PD, Holmes GL, Hickey PR, Strand RD et al (1995) Developmental and neurologic status of children after heart surgery with hypothermic circulatory arrest or low-flow cardiopulmonary bypass. N Engl J Med 332:549–555
3. Berg C, Gembruch O, Gembruch U, Geipel A (2009) Doppler indices of the middle cerebral artery in fetuses with cardiac defects theoretically associated with impaired cerebral oxygen delivery in utero: is there a brain-sparing effect? Ultrasound Obstet Gynecol 34:666–672
4. Donofrio MT, Bremer YA, Schieken RM, Gennings C, Morton LD, Eidem BW, Cetta F, Falkensammer CB, Huhta JC, Kleinman CS (2003) Autoregulation of cerebral blood flow in fetuses with congenital heart disease: the brain sparing effect. Pediatr Cardiol 24:436–443
5. Gramellini D, Folli MC, Raboni S, Vadora E, Merialdi A (1992) Cerebral-umbilical Doppler ratio as a predictor of adverse perinatal outcome. Obstetr Gynecol 79:416–420
6. Johnston MV (2007) Congenital heart disease and brain injury. N Engl J Med 357:1971–1973
7. Jouannic JM, Benachi A, Bonnet D, Fermont L, Le Bidois J, Dumez Y, Dommergues M (2002) Middle cerebral artery Doppler in fetuses with transposition of the great arteries. Ultrasound Obstet Gynecol 20:122–124

8. Kaltman JR, Di H, Tian Z, Rychik J (2005) Impact of congenital heart disease on cerebrovascular blood flow dynamics in the fetus. Ultrasound Obstet Gynecol 25:32–36
9. Licht DJ, Shera DM, Clancy RR, Wernovsky G, Montenegro LM, Nicolson SC, Zimmerman RA, Spray TL, Gaynor JW, Vossough A (2009) Brain maturation is delayed in infants with complex congenital heart defects. J Thorac Cardiovasc Surg 137:529–536; discussion 536–527
10. Limperopoulos C, Majnemer A, Shevell MI, Rosenblatt B, Rohlicek C, Tchervenkov C (1999) Neurologic status of newborns with congenital heart defects before open heart surgery. Pediatrics 103:402–408
11. Limperopoulos C, Majnemer A, Shevell MI, Rohlicek C, Rosenblatt B, Tchervenkov C, Darwish HZ (2002) Predictors of developmental disabilities after open heart surgery in young children with congenital heart defects. J Pediatr 141:51–58
12. Maeno YV, Kamenir SA, Sinclair B, van der Velde ME, Smallhorn JF, Hornberger LK (1999) Prenatal features of ductus arteriosus constriction and restrictive foramen ovale in d-transposition of the great arteries. Circulation 99:1209–1214
13. Manzar S, Nair AK, Pai MG, Al-Khusaiby SM (2005) Head size at birth in neonates with transposition of great arteries and hypoplastic left heart syndrome. Saudi Med J 26:453–456
14. Massaro AN, El-Dib M, Glass P, Aly H (2008) Factors associated with adverse neurodevelopmental outcomes in infants with congenital heart disease. Brain Dev 30:437–446
15. Meise C, Germer U, Gembruch U (2001) Arterial Doppler ultrasound in 115 second- and third-trimester fetuses with congenital heart disease. Ultrasound Obstet Gynecol 17:398–402
16. Rosenthal GL (1996) Patterns of prenatal growth among infants with cardiovascular malformations: possible fetal hemodynamic effects. Am J Epidemiol 143:505–513
17. Rudolph AM (1985) Distribution and regulation of blood flow in the fetal and neonatal lamb. Circ Res 57:811–821
18. Rudolph AM (2007) Aortopulmonary transposition in the fetus: speculation on pathophysiology and therapy. Pediatr Res 61:375–380
19. Rudolph AM, Heymann MA (1967) The circulation of the fetus in utero: methods for studying distribution of blood flow, cardiac output and organ blood flow. Circ Res 21:163–184
20. Saiki H, Kurishima C, Masutani S, Tamura M, Senzaki H (2013) Impaired cerebral perfusion after bilateral pulmonary arterial banding in patients with hypoplastic left heart syndrome. Ann Thor Surg 96:1382–1388
21. Shillingford AJ, Ittenbach RF, Marino BS, Rychik J, Clancy RR, Spray TL, Gaynor JW, Wernovsky G (2007) Aortic morphometry and microcephaly in hypoplastic left heart syndrome. Cardiol Young 17:189–195
22. van Houten JP, Rothman A, Bejar R (1996) High incidence of cranial ultrasound abnormalities in full-term infants with congenital heart disease. Am J Perinatol 13:47–53

PEDIATRICS INTERNATIONAL Official Journal of the Japan Pediatric Society

Pediatrics International (2015) **57**, 189–192 doi: 10.1111/ped.12584

Brief Report

Drug treatment for bronchopulmonary dysplasia in Japan: Questionnaire survey

Ryo Ogawa,[1] Rintaro Mori,[2] Mayumi Sako,[3] Misao Kageyama,[4] Masanori Tamura[1] and Fumihiko Namba[1]

[1]*Department of Pediatrics, Saitama Medical Center, Saitama Medical University, Saitama,* [2]*Department of Health Policy,* [3]*Division of Clinical Trials, Clinical Research Center, National Center for Child Health and Development, Tokyo and* [4]*Department of Neonatology, Okayama Medical Center, Okayama, Japan*

Abstract Bronchopulmonary dysplasia (BPD) is one of the most common complications in premature infants. Although several different drugs have been developed for BPD, there is a wide variation in the choice of drug used among facilities. The aim of this study was to carry out a survey of the current drugs used to treat BPD in Japan. Questionnaires regarding the current use of drugs for BPD were sent to tertiary neonatal units. The response rate was 80% (77/96). Most units used antenatal steroids and oral diuretics for the prevention and treatment of BPD, respectively. Only 4% used caffeine for prevention, whereas 88% used systemic corticosteroids for treatment. Few units used inhaled anticholinergics and i.v. vitamins for the prevention and treatment of BPD, respectively. It was found that the drugs used to treat BPD vary greatly among institutions. Further research is required to develop evidence-based clinical guidelines for BPD in premature infants.

Key words bronchopulmonary dysplasia, caffeine, drug, questionnaire, steroid.

Bronchopulmonary dysplasia (BPD), also known as a chronic lung disease of infancy, was first described by Northway *et al.* in 1967.[1] Despite ongoing studies to improve neonatal respiratory care, including exogenous surfactant therapy and the use of antenatal steroids, BPD continues to carry a considerable risk of mortality and long-term morbidity. Several devices and strategies, such as nasal continuous positive airway pressure, high frequency oscillatory ventilation, and permissive hypercapnia, have been developed to improve the respiratory outcome of newborns. In addition, several drugs have been used in an attempt to prevent BPD or treat established BPD. Although there is considerable evidence to support the routine use of some drugs, most drug treatment is still individual or institution specific, according to the personal experiences and beliefs of physicians. Therefore, the aim of this study was to survey current practices in Japan regarding the drugs used for the prevention and treatment of BPD and determine whether their use is evidence based.

Methods

A questionnaire was sent to all 96 tertiary neonatal units in Japan. Data were collected between August 2013 and September 2013. Questions were asked on the policies of the neonatal units regarding which drugs were currently used or had been used in the past for the prevention and treatment of BPD. Each question included choice of drug prescribed, which required either a yes or no response together with blank spaces in which the respondents filled in the specific name of a drug. In addition, respondents were given the option of naming drugs not described in the list. BPD was defined as oxygen dependence at 28 days of age. "Preventative therapy" referred to the use of a drug before the diagnosis of BPD on day 28, whereas "treatment" referred to the use of a drug after the diagnosis of BPD.

Results

There was an 80% (77/96) response rate to the questionnaire. The units responding to the questionnaire were distributed evenly from Hokkaido to Okinawa, from the north to the south of Japan, respectively (Fig. 1). A total of 87% of the units used antenatal steroids to prevent BPD, which is known to prevent respiratory distress syndrome (RDS) by accelerating fetal lung maturation (Fig. 2a). Among the antenatal steroids used to prevent BPD, betamethasone was given in 97% of the units, whereas dexamethasone was used only in 3% (Fig. 3a). Oral diuretics, most commonly furosemide and spironolactone, were used in 84% of the units for the treatment of BPD (Fig. 2b). Several drugs were used in <10% of the units, such as β-stimulators and anticholinergic agents for the prevention of BPD, and protease inhibitors and antioxidants for the treatment of BPD. These were considered to be institution-specific practices without any evidence (Fig. 2). Oral xanthine derivatives were used for the prevention of BPD in 42% of the units, but caffeine therapy

Correspondence: Fumihiko Namba, MD PhD, Department of Pediatrics, Saitama Medical Center, Saitama Medical University, 1981 Kamoda, Kawagoe, Saitama 350-8550, Japan. Email: nambaf@saitama-med.ac.jp.

Received 7 August 2014; revised 28 October 2014; accepted 17 December 2014.

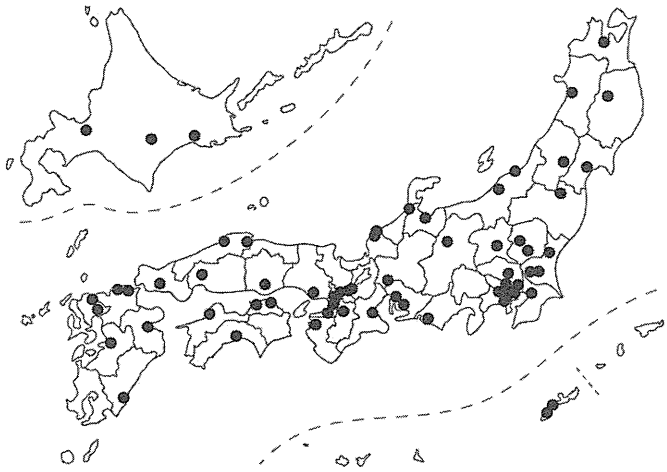

Fig. 1 Tertiary neonatal units in Japan that responded to the questionnaire. Response rate was 80% (77/96).

was offered in only 13% of these units, and theophylline and aminophylline were used in 72% and 16%, respectively (Fig. 2). Vitamin A was used for the prevention of BPD in only 8% of the units (Fig. 2a). The use of early (<28 days of life) and delayed/late (≥28 days of life) systemic corticosteroids (i.v. or p.o.) occurred in 35% and 88% of units, respectively (Fig. 2). Hydrocortisone was used as an early systemic corticosteroid in 70% of units, whereas dexamethasone was used in 21% after evidence had been established that more adverse neurodevelopmental outcomes occur following early systemic dexamethasone therapy (Fig. 3b).[2] Delayed/late systemic corticosteroids, including hydrocortisone (85%) and dexamethasone (53%), were used to treat BPD in 89% of the units (Figs 2b, 3d).

Discussion

This is the first Japanese survey of the drugs used to prevent and treat BPD. The response rate was generally good.

This survey showed that most units use antenatal corticosteroids to prevent BPD. The use of a single course of corticosteroids in a mother who is in preterm labor to accelerate the maturation of the surfactant system in the fetal lungs is considered safe. Although this reduces mortality and the risk of RDS, there is no evidence that it reduces the risk of BPD, probably because of an increase in survival.[3] The use of multiple courses of antenatal corticosteroids significantly increased the risk of BPD, but systematic review comparing the use of multiple courses with a single course did not show any difference in the risk of BPD.[3] Although there is no evidence to support the efficacy of antenatal corticosteroid therapy in BPD, antenatal corticosteroids are used to prevent BPD in Japan. This may be because RDS is one of the most common risk factors for the development of BPD.

Caffeine is a methylxanthine that is commonly used to treat apnea of prematurity.[4] Methylxanthines reduce the frequency of apnea of prematurity and the need for mechanical ventilation during the first 7 days of treatment.[5] A recent large randomized controlled trial followed the primary outcome of long-term neurodevelopment, and secondary outcome of short-term BPD rate in infants with birthweight 500–1250 g.[5] A total of 36% of the infants in the caffeine-treated group had BPD compared with 47% in the placebo group.[5] The mechanism by which caffeine decreases the incidence of BPD, however, remains unknown. Nevertheless, current evidence supports the use of caffeine for the treatment of apnea of prematurity and also suggests that it exerts secondary benefits including a reduction in the rate of BPD. Despite the utility of caffeine for the prevention of BPD, only 4% of the units that responded to the survey in the current

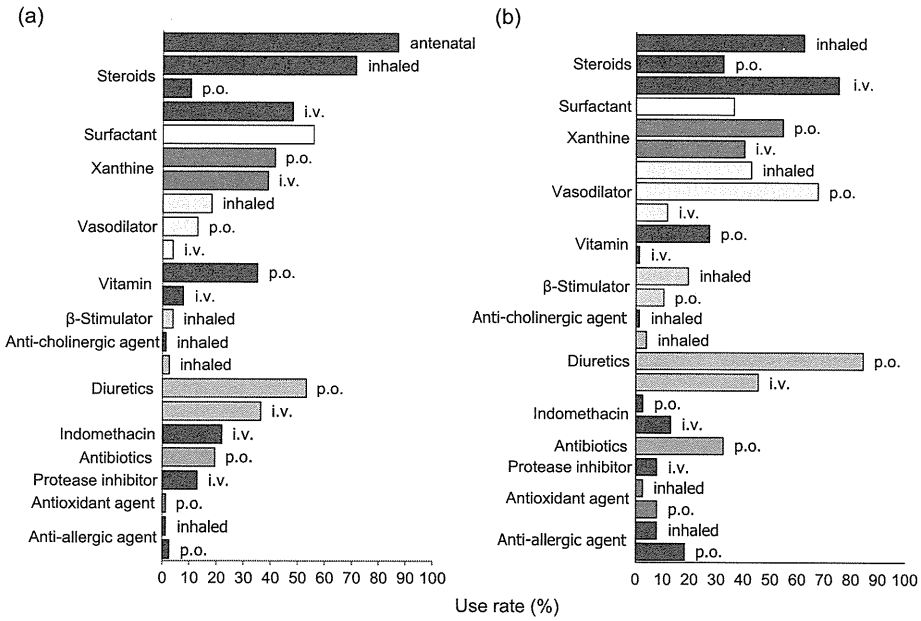

Fig. 2 Drugs for (a) prevention (i.e. before diagnosis on day 28) and (b) treatment (i.e. after diagnosis on day 28) of bronchopulmonary dysplasia in Japan.

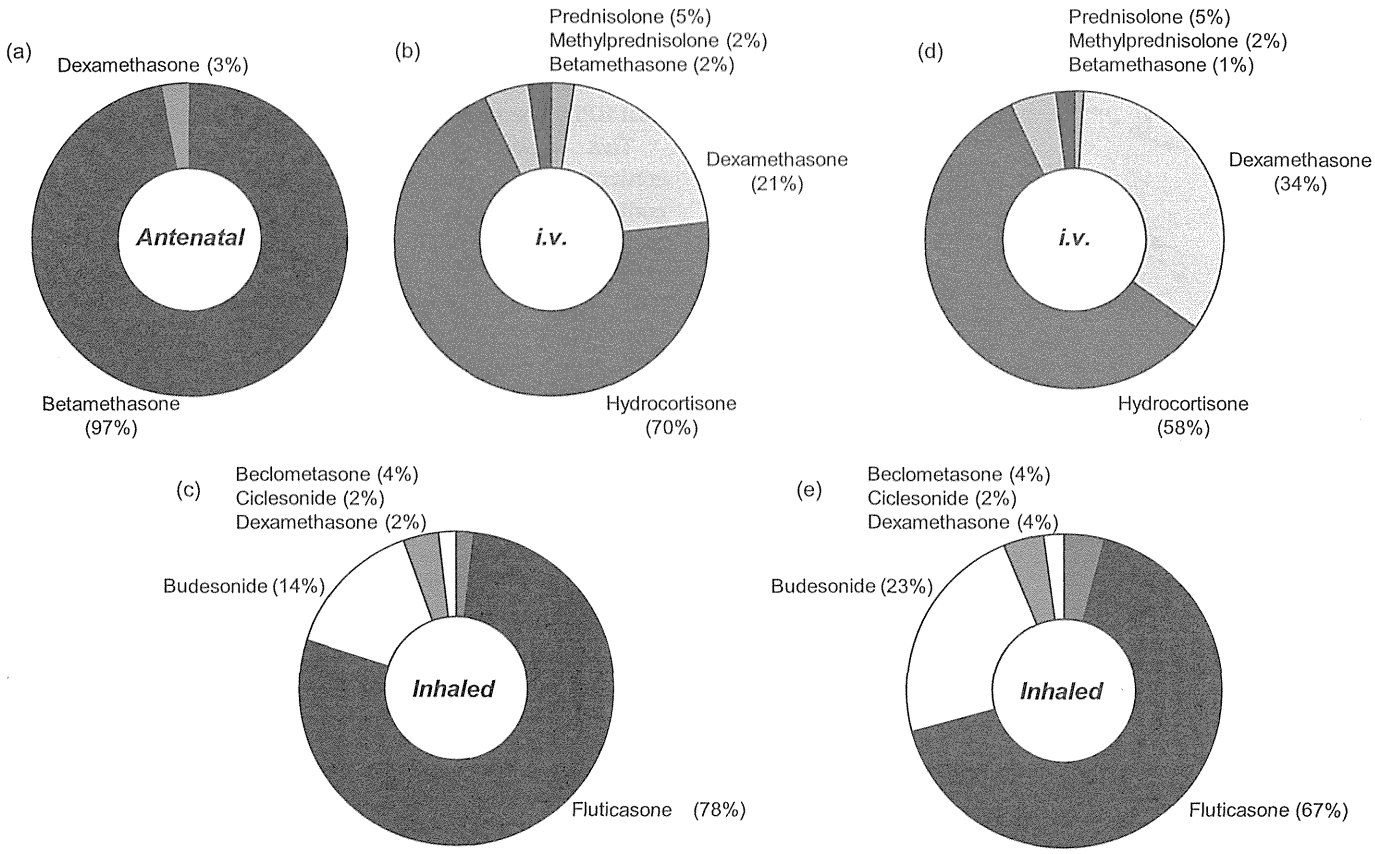

Fig. 3 Steroids for (a–c) prevention (before diagnosis on day 28) and (d,e) treatment (after diagnosis on day 28) of bronchopulmonary dysplasia in Japan.

study used caffeine to prevent the development of BPD. This is because caffeine citrate is not approved for use in Japan, even though it is approved in at least 38 countries worldwide, including the USA and European countries. Caffeine citrate is only one drug that can be used in the treatment of apnea of prematurity listed in "WHO Model List of Essential Medicines for Children".[6] Caffeine citrate is currently under review for drug registration in Japan and is likely to be approved for use in 2014. A reduction in the rate of BPD is expected after the use of caffeine citrate has been approved.

A Cochrane meta-analysis of randomized controlled trials to evaluate the effects of early dexamethasone treatment (<8 days after birth) on the incidence of BPD, found that steroids facilitated extubation and decreased the incidence of BPD.[2] Adverse effects, however, such as hyperglycemia, gastrointestinal perforation, hypertension, infection, steroid-induced cardiomyopathy, and long-term neurodevelopmental effects including cerebral palsy were observed.[2] In the present survey, dexamethasone was used for the prevention of BPD in 30% of cases that involved systemic corticosteroids. Although it is unknown whether dexamethasone was used early (within 7 days of birth) in those patients, 30% still appears to be a high use rate. Secondary questionnaire are required to determine the date that dexamethasone was given, and stern warnings should be issued to the units that administered dexamethasone soon after delivery.

A small number of units used inhaled anticholinergic, oral expectorants, and inhaled disodium cromoglycate for the prevention of BPD, whereas i.v. vitamin, inhaled anticholinergic, and inhaled antioxidant were used for the treatment of BPD. Most of these may represent cases of drug misuse because of a lack of evidence for the efficacy of these agents in BPD or because of their very institution-specific use; therefore, appropriate clinical studies or guidelines are required.

Conclusion

This is the first Japanese survey of the drugs used to prevent and treat BPD, and it achieved a good response rate. The present survey provides information on the heterogeneity of treatment practices for BPD in the participating centers. The survey confirms the misuse of some drugs, and thereby highlights the importance of the formulation and dissemination of evidence-based guidelines for the prevention and treatment of BPD.

Acknowledgments

Dr Namba is supported by Young Investigator Grant from Kawano Masanori Memorial Public Interest Incorporated Foundation for Promotion of Pediatrics, Saitama Medical University Internal Research Grant from Saitama Medical University, and Health Labour Sciences Research Grant, "Studies to elucidate the

pathogenesis and long-term outcomes of low birthweight infants" from the Ministry of Health Labour and Welfare.

References

1 Northway WH, Rosan RC, Porter DY. Pulmonary disease following respirator therapy of hyaline-membrane disease. Bronchopulmonary dysplasia. *N. Engl. J. Med.* 1967; **276**: 357–68.
2 Doyle LW, Ehrenkranz RA, Halliday HL. Early (<8 days) postnatal corticosteroids for preventing chronic lung disease in preterm infants. *Cochrane Database Syst. Rev.* 2014; (5): CD001146.
3 Crowley P. Prophylactic corticosteroids for preterm birth. *Cochrane Database Syst. Rev.* 2000; (2): CD000065.
4 Henderson-Smart DJ, Steer P. Methylxanthine treatment for apnea in preterm infants. *Cochrane Database Syst. Rev.* 2001; (3): CD000140.
5 Schmidt B, Roberts RS, Davis P *et al.* Caffeine therapy for apnea of prematurity. *N. Engl. J. Med.* 2006; **354**: 2112–21.
6 *WHO Model List of Essential Medicines for Children*, 4th edn. 2013. [Cited April 2013.] Available at: http://www.who.int/medicines/publications/essentialmedicines/en/.

Surg Today (2014) 44:761–766
DOI 10.1007/s00595-013-0565-x

CASE REPORT

Thoracoscopy-assisted removal of a thoracoamniotic shunt double-basket catheter dislodged into the fetal thoracic cavity: report of three cases

Seiichiro Inoue · Akio Odaka · Kazunori Baba · Tetsuya Kunikata · Hisanori Sobajima · Masanori Tamura

Received: 1 June 2012 / Accepted: 24 September 2012 / Published online: 28 March 2013

Abstract The indications for and timing of surgical removal of a dislodged thoracoamniotic shunt double-basket catheter are not established, and the side effects of the dislodged into the thoracic cavity remain controversial. The double-basket catheter was designed to reduce the incidence of catheter dislodgement; however, we have encountered four cases of thoracoamniotic shunt double-basket catheter dislodgement into the fetal thorax. The dislodged shunt catheters were removed safely with thoracoscopic assistance within several days of birth, when additional treatments for pleural effusion were needed, such as thoracic drainage tube insertion and adhesion treatment of the thorax. We report the clinical courses of three of these cases of thoracoamniotic shunt tube dislocation. By waiting several days postnatally for stabilization of respiratory and circulatory status and the effective use of thoracoscopic assistance, the dislodged catheter was safely removed from the neonatal thorax. The accumulation of case reports will help establish suitable treatments, and their indication, for a dislodged thoracoamniotic shunt catheter within the fetal thoracic cavity.

S. Inoue (✉) · A. Odaka
Department of Hepato-Billiary-Pancreatic and Pediatric Surgery, Saitama Medical Center, Saitama Medical University, Kamoda 1981, Kawagoe, Saitama 3508550, Japan
e-mail: sei_khsr@saitama-med.ac.jp

K. Baba
Department of Obstetrics and Gynecology, Saitama Medical Center, Saitama Medical University, Kamoda 1981, Kawagoe, Saitama 3508550, Japan

T. Kunikata · H. Sobajima · M. Tamura
Department of Pediatrics, Saitama Medical Center, Saitama Medical University, Kamoda 1981, Kawagoe, Saitama 3508550, Japan

Keywords Thoracoamniotic shunt · Catheter dislodgement · Double-basket catheter · Thoracoscopic removal

Introduction

Thoracoamniotic shunting is an effective treatment for massive pleural effusion and intrathoracic cystic disease in the fetus [1–3]. Massive pleural effusion or an intrathoracic mass may increase intrathoracic pressure, compress the lung and disturb normal lung development [4]. Moreover, an intrathoracic mass or pleural effusion displaces mediastinal structures, inducing hemodynamic changes and increasing the risk of hydrops.

Dislodgement of a catheter into the fetal thoracic cavity, caused by a decrease in either fetal pleural effusion or fetal growth, is an important complication. We report three cases of intrathoracic dislodgement of a thoracoamniotic shunt double-basket catheter, which was surgically removed when aspiration tube insertion or adhesion treatment of thorax was needed. The dislodged catheter was removed safely with thoracoscopic assistance after delivery. Following these case reports, we discuss the suitable treatment of thoracoamniotic shunt catheter dislodgement into the thoracic cavity.

Case reports

Between 2007 and 2011, we inserted 20 thoracoamniotic shunt tubes and encountered four cases of shunt tube dislocation into the fetal thorax (Tables 1, 2). We report the clinical course of cases 1, 2, and 3.

Table 1 Profiles of the four babies with thoracoamniotic shunt tube dislocation (1)

Case	Sex	Reason for fetal pleural effusion	Diagnosis of fetal pleural effusion	1st thoracoamniotic shunt tube insertion
1	F	Congenital chylothorax	34w0d	34w5d
2	F	Congenital chylothorax	31w5d	32w0d
3	M	Congenital chylothorax	29w6d	31w1d
4	F	Congenital chylothorax	21w2d	33w4d

Table 2 Profiles of the babies with thoracoamniotic shunt tube dislocation (2)

Case	Delivery	Birth	Birth weight (g)	Apgar score (1/5 min)	Operation (days after birth)	Discharge (days after birth)
1	C/S	35w4d	2720	6/8	3	41
2	Vaginal	37w0d	2926	2/4	0	43
3	Vaginal	35w3d	2632	5/8	6	74
4	Vaginal	40w2d	3680	9/9	0	35

C/S cesarean section

Case 1

A baby girl was delivered at 35 weeks and 4 days gestation by cesarean section because of early amniorrhexis, after massive bilateral pleural effusion, ascites, and hydramnios had been detected by fetal ultrasound examination at 34 weeks gestation. Fetal lung hypoplasia was not detected. We aspirated the fetal pleural effusion and ascites; however, massive pleural effusion was detected again the following day. To prevent exacerbation of hydrops, we inserted thoracoamniotic shunts with double-basket catheters: two in the right thorax and one in the left.

The shunt catheter inserted into the left thorax was removed at delivery, but that inserted into the right thorax could not be found. Her respiratory condition was unstable and chest radiography revealed massive pleural effusion and two dislodged shunt tubes. We aspirated 110 ml of right pleural effusion 2 h after delivery (Fig. 1a), but massive right pleural effusion developed again within 3 days postnatally. Thus, we inserted a chest drainage tube and removed the dislodged shunt catheters, with thoracoscopic assistance to avoid infection of the thorax. Thoracoscopy was performed through a small window thoracotomy incision in right chest wall. Both shunt catheters were found behind the lower lobe of the right lung and we removed them using forceps inserted through the same incision (Fig. 1b). A chest drainage tube was then inserted through the same incision. The postoperative course was uneventful and the baby was discharged 41 days postnatally.

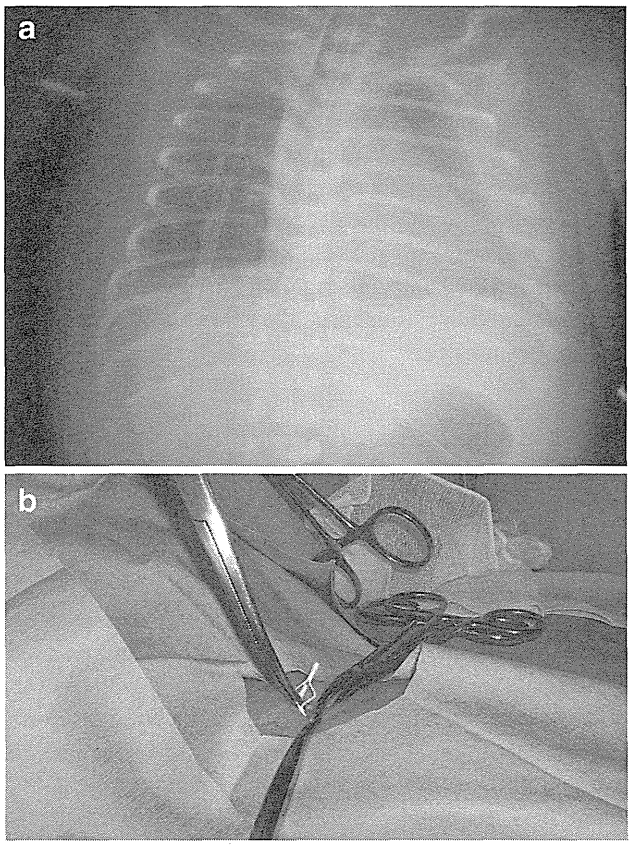

Fig. 1 Case 1: chest X-ray after aspiration of the right pleural effusion (**a**) and photograph of a surgically removed dislodged thoracoamniotic shunt catheter (**b**). Two dislodged shunt catheters in the right thorax were detected by chest radiography. Right pleural effusion was completely aspirated 2-h after delivery (**a**). The catheters were removed safely through a small surgical incision (**b**)

Case 2

A baby girl was delivered at 37 weeks gestation by normal vaginal delivery.

At 31 weeks and 5 days gestation, hydramnios and fetal pleural effusion had been detected by fetal ultrasonography. Although the hypoplasia of the fetal lung was not

severed, at 32 weeks gestation we inserted thoracoamniotic shunt catheters (one in the right thorax and two in the left), to prevent mediastinal shift or caval compression. By 35 weeks and 1 day gestation, the right pleural effusion had increased and dislodgement of one of the shunt catheters into the right thorax was detected by ultrasound examination (Fig. 2a). Another pleuroamniotic shunt catheter was inserted into the right thorax; however, by 36 weeks and 3 days gestation, the right pleural effusion had increased again. Immediately after delivery, the baby was intubated and mechanical ventilation was started. One shunt catheter was found in each chest wall, both of which were removed at birth. The tip of a third catheter was palpable subcutaneously over the left chest wall and a fourth was detected in the right thorax, by radiography. Using thoracoscopy-assisted surgery, we removed the shunt catheter and inserted a chest drainage tube on the day of delivery. The thoracoscope was inserted through a small thoracotomy incision in the right chest wall, revealing massive pleural effusion and a dislodged shunt catheter between the middle and lower lobes of the right lung. Under thoracoscopic observation, a suction tube was inserted and the shunt catheter was aspirated with the pleural effusion. Another catheter, the tip of which had been detected subcutaneously, was removed through small skin incision near the tip of the tube. A chest drainage tube was then inserted into the right chest. The postoperative course was uneventful, and the baby was discharged 43 days postnatally.

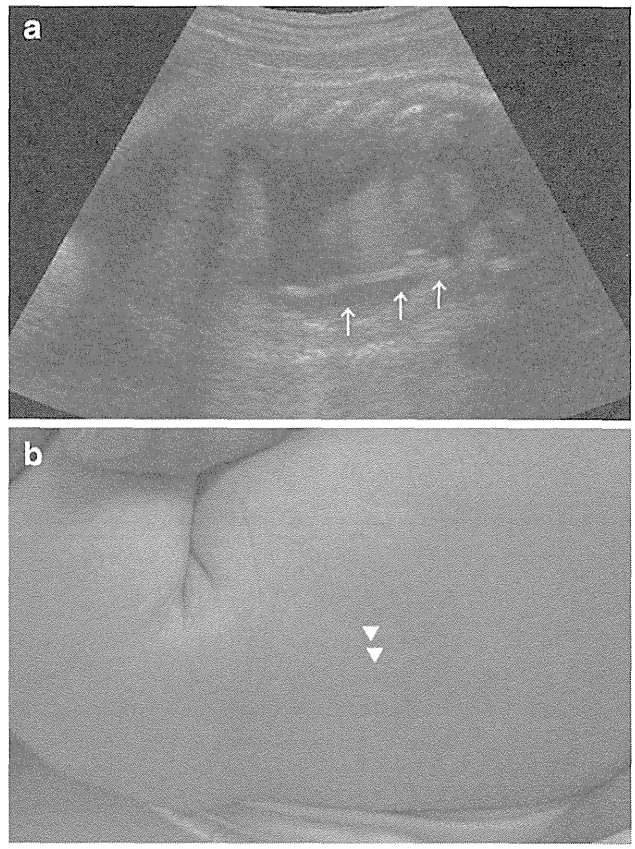

Fig. 2 Case 2: fetal ultrasound at 35 weeks and 1 day gestation (**a**) and photograph of the chest scar 2 months postoperatively (**b**). The dislodged catheter in the fetal right thorax was clearly seen on the ultrasound image (↑) (**a**). The scar following shunt catheter removal was cosmetically satisfactory (△) (**b**)

Case 3

A baby boy was delivered vaginally at 35 weeks and 3 days gestation.

At 29 weeks and 6 days gestation, bilateral pleural effusion had been detected in the fetus and at 30 weeks and 2 days gestation, right pleural effusion was aspirated and chylothorax diagnosed. By 31 weeks and 1 day gestation, re-accumulation of the right pleural effusion was detected by ultrasound, although the lung hypoplasia was not severe. A thoracoamniotic shunt catheter was inserted to prevent hydrops. Between 32 and 34 weeks gestation, a total of 5 double-basket catheters were inserted, one of which dislodged into the mother's uterus. At 35 weeks and 2 days gestation, labor pains started and amniorrhexis was observed. At delivery, the shunt catheter found in the right chest wall was removed. The other 3 catheters were detected later in the right chest, by radiography (Fig. 3a). We inserted an aspiration tube into his right chest cavity and drained the pleural effusion. On day 4 postnatally, chest computed tomography showed the three shunt catheters in the right thorax. The tip of one catheter was buried in the right chest wall (Fig. 3b–d).

On day 6 postnatally, the dislodged shunt catheters were surgically removed to allow adhesion therapy to be started for chylothorax. A small skin incision was made over the site where one shunt catheter was palpable below the skin and the catheter was removed. A small thoracotomy incision was made by extension of where the chest drainage tube had been inserted in the right chest wall, along with the thoracoscope. Massive pleural effusion and fibrin were observed. A second dislodged shunt catheter was found thoracoscopically and removed using forceps inserted through the incision (Fig. 4a). The third catheter was difficult to see thoracoscopically because it was completely enveloped in a fibrin sheath. After removal of this fibrin sheath, the catheter was gently tracked using forceps (Fig. 4b). However, it could not be removed because tip was buried within the chest wall. The thoracotomy incision was enlarged to 3 cm, and the catheter was tracked and removed. A chest drainage tube was then inserted. After surgical removal of this shunt catheter, massive pleural effusion persisted and intrathoracic minomycin (×3), OK-432 (×2), and intravenous octreotide were administered.

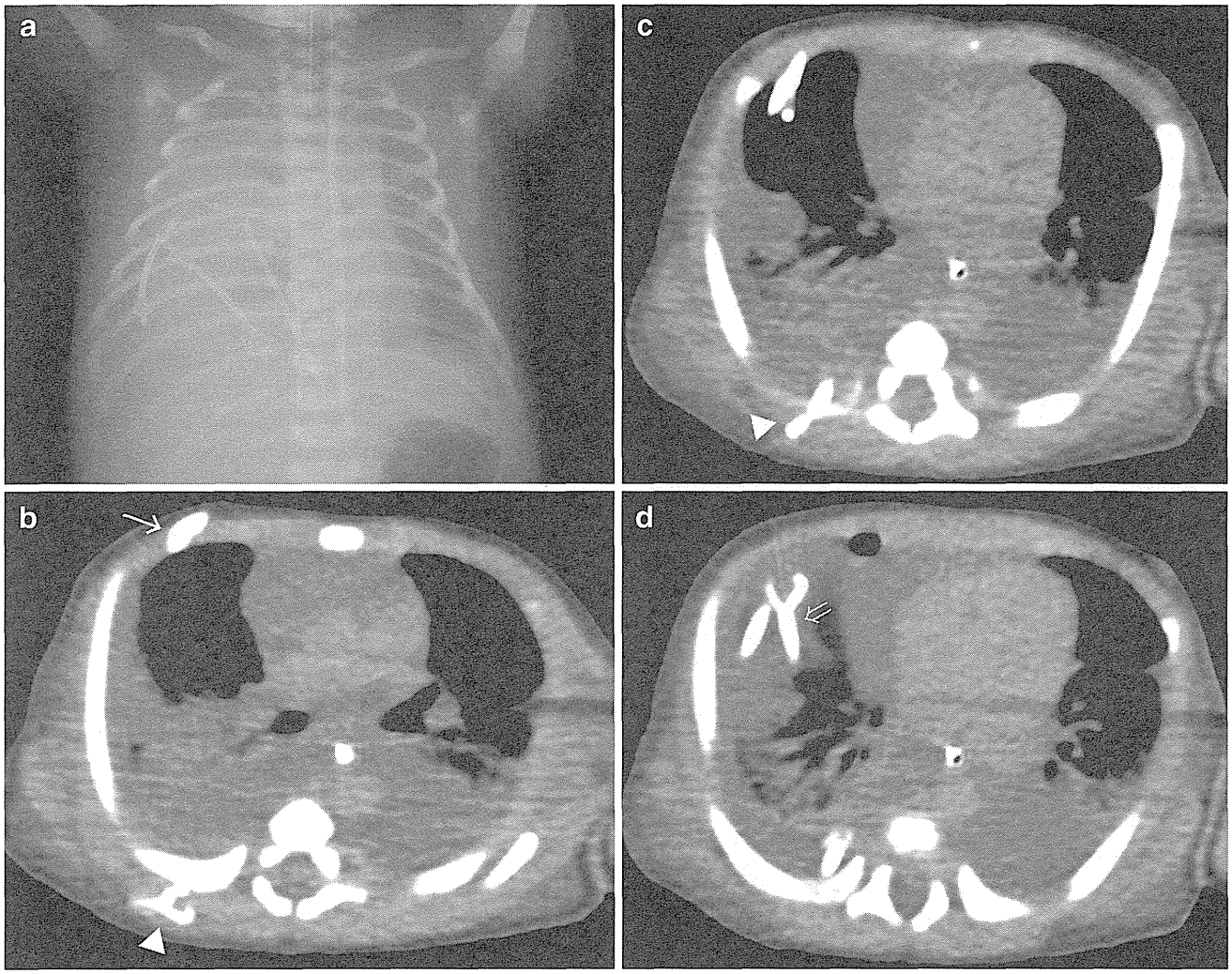

Fig. 3 Case 3: chest X-ray at delivery (**a**) and chest computed tomography on day 4 postnatally (**b–d**). The three dislodged shunt catheters in the right thorax were detected radiographically at delivery (**a**). The catheter that was palpable subcutaneously (⇩) was removed through a small skin incision (**b**). The tip of a second catheter was buried within the chest wall (▼) and enveloped by a fibrin sheath (**c**). The third catheter was found (⇒) and removed with thoracoscopic assistance (**d**)

During this treatment regimen, the chest drainage tube was removed and re-inserted twice because of obstruction by the aspirated fibrin. After removal of the drainage tube, no re-accumulation of effusion was observed and the baby was discharged 74 days postnatally.

Discussion

Fetal thoracoamniotic shunting is an intrauterine intervention done for massive fetal pleural effusion [4–7] and fetal intrathoracic cystic lesions such as congenital cystic adenomatoid malformation and pulmonary sequestration, which may reduce perinatal morbidity and mortality [1, 8]. While double pigtail catheters have often been used for pleuroamniotic shunting [1–3], Sase et al. and Murabayashi et al. [5, 6] reported that they can be difficult to insert into the early fetal intrathoracic cavity because of their length and because they are not easy to see on ultrasonography. The double-basket catheter is considered superior because of its suitable length, straight conformation, and easy visualization on ultrasonography. Sase et al. [5] also mentioned that the double-basket catheter does not dislodge as easily.

In our center, the double-basket catheter is used for fetal pleuroamniotic shunting; however, we have been encountered four cases of dislodgement of double-basket catheters into the fetal thoracic cavity, after their insertion at 31–34 weeks gestation for the purpose of reducing fetal pleural effusion and preventing hydrops. Thus, the timing of catheter insertion, the purpose of shunting, and catheter selection should be discussed to establish the most appropriate treatment for fetal pleural effusion.

The indications for surgical removal are controversial. Sepulveda et al. and Alkazaleh et al. reported cases of

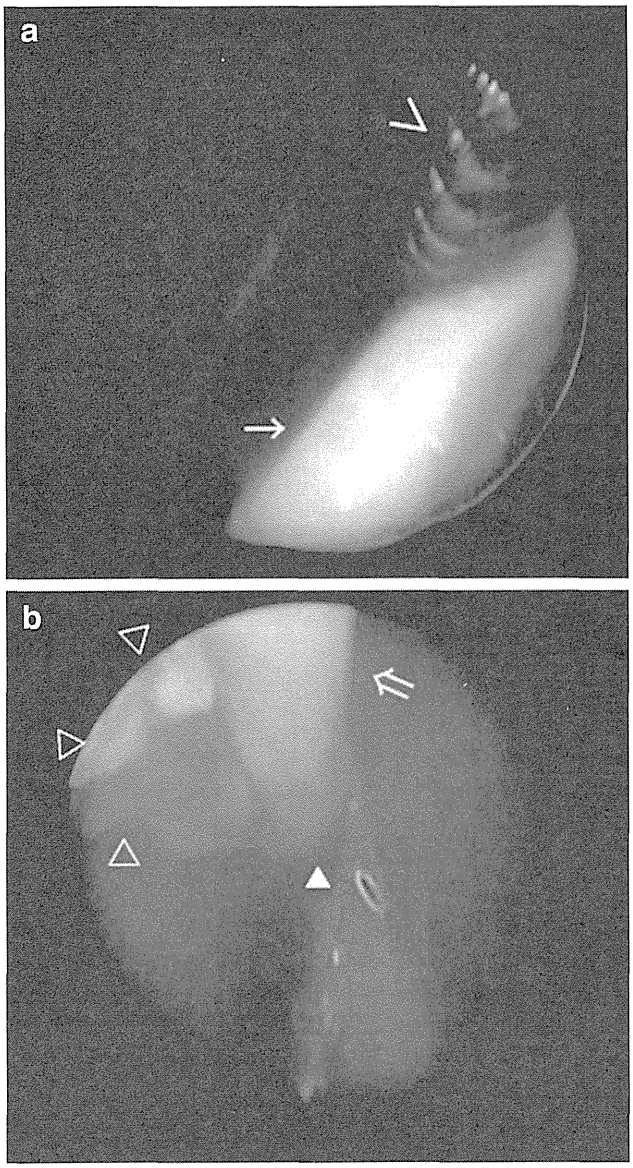

Fig. 4 Case 3: photograph of the thoracoscopy. The second dislodged shunt catheter (⇓) was removed using forceps (⋁) inserted through the same thoracoscopy incision (**a**). After partial removal of the fibrin sheath (△), the third catheter (⇒) was found thoracoscopically, but its tip was buried within the chest wall (▲) (**b**)

dislodged pigtail catheters that were followed-up 24 and 12 months, postnatally, respectively. Both reports stated that a dislodged catheter should not cause long-term pulmonary complications and that a conservative approach might be the most sensible management option [9, 10]. However, Blanch et al. reported a case of shunt catheter dislodgement resulting in compression of the lung hilum causing death on day 6 postnatally [11]. We decided to surgically remove the dislodged catheters in our patients because of the massive pleural effusions requiring postnatal intervention. We worried about the risk of infection associated with the continuous drainage of pleural effusion that was needed. In particular, when adhesion therapy for massive infantile pleural effusion is needed postnatally, as with case 3, the effects of a double-basket catheter on adhesion therapy are thought to be unpredictable. An accumulation of case reports of conservative treatment for not only the double pigtail catheter but also the double-basket catheter is needed to clarify this.

The value of thoracoscopic intervention for adult massive pleural effusion is well documented [12]. We performed surgical removal with thoracoscopic assistance postnatally. After making a small incision in the chest wall, the area is inspected prior to any aggressive aspiration. When using the thoracoscope, the presence of pleural effusion sometimes assists in locating the dislodged tube because it creates a space between the chest wall and the lung or interlobar fissure for insertion of the thoracoscope. Moreover, when the catheter is located in an awkward site, such as in the interlobar fissure and is difficult to remove using forceps, we aspirate the catheter along with the pleural effusion, as in our case 2. Figure 2b shows the good cosmetic results after thoracoscopically assisted shunt catheter removal via a small thoracotomy incision.

When the catheter is difficult to remove safely, we extend the incision and confirm the location of the catheter directly. In case 3, the shunt catheter was completely enveloped by fibrin sheath and it could not be located thoracoscopically. Moreover, the tip of the double-basket catheter was buried within the muscle layer of the chest wall and was not palpable. When the tip of the catheter is palpable subcutaneously, it is easy to make a skin incision over it and remove it directly. Hence, we enlarged the incision and opened the chest wall further to see the catheter directly, and remove it from the thoracic cavity. Initial thoracoscopic observation and enlargement of the thoracotomy incision may assist in performing open removal safely via a minimal incision.

Conflict of interest We declare that no conflicts of interest associated with this report.

References

1. Adzick NS, Harrison MR, Crombleholme TM, Flake AW, Howell LJ. Fetal lung lesions: management and outcome. Am J Obstet Gynecol. 1998;179(4):884–9.
2. Smith RP, Illanes S, Denbow ML, Soothill PW. Outcome of fetal pleural effusions treated by thoracoamniotic shunting. Ultrasound Obstet Gynecol. 2005;26(1):63–6.
3. Bianchi S, Lista G, Castoldi F, Rustico M. Congenital primary hydrothorax: effect of thoracoamniotic shunting on neonatal clinical outcome. J Matern Fetal Neonatal Med. 2010;23(10):1225–9.
4. Rodeck CH, Fisk NM, Fraser DI, Nicolini U. Long-term in utero drainage of fetal hydrothorax. N Engl J Med. 1988;319(17):1135–8.

5. Sase M, Miwa I, Hasegawa K, Sumie M, Nakata M, Kato H. Successful treatment of primary fetal hydrothorax with a double basket catheter. Am J Perinatol. 2002;19(8):405–12.
6. Murabayashi N, Sugiyama T, Kusaka H, Sagawa N. Thoracoamniotic shunting with double-basket catheters for fetal chylothorax in the second trimester. Fetal Diagn Ther. 2007;22(6):425–7.
7. Yinon Y, Grisaru-Granovsky S, Chaddha V, Windrim R, Seaward PG, Kelly EN, et al. Perinatal outcome following fetal chest shunt insertion for pleural effusion. Ultrasound Obstet Gynecol. 2010;36(1):58–64.
8. Becmeur F, Horta-Geraud P, Donato L, Sauvage P. Pulmonary sequestrations: prenatal ultrasound diagnosis, treatment, and outcome. J Pediatr Surg. 1998;33(3):492–6.
9. Sepulveda W, Galindo A, Sosa A, Diaz L, Flores X, de la Fuente P. Intrathoracic dislodgement of pleuro-amniotic shunt. Three case reports with long-term follow-up. Fetal Diagn Ther. 2005;20(2):102–5.
10. Alkazaleh F, Saleem M, Badran E. Intrathoracic displacement of pleuroamniotic shunt after successful in utero treatment of fetal hydrops secondary to hydrothorax. Case report and review of the literature. Fetal Diagn Ther. 2009;25(1):40–3.
11. Blanch G, Walkinshaw SA, Hawdon JM, Weindling AM, van Velzen D, Rodeck CH. Internalization of pleuroamniotic shunt causing neonatal demise. Fetal Diagn Ther. 1996;1(11):32–6.
12. Kamiyoshihara M, Ibe T, Kakegawa S, et al. Late-onset chylothorax after blunt chest trauma at an interval of 20 years: report of a case. Surg Today. 2008;38:56–8.

Heart Vessels (2014) 29:825–833
DOI 10.1007/s00380-013-0422-2

ORIGINAL ARTICLE

Assessment of ventricular relaxation and stiffness using early diastolic mitral annular and inflow velocities in pediatric patients with heart disease

Satoshi Masutani · Hirofumi Saiki · Clara Kurishima · Seiko Kuwata · Masanori Tamura · Hideaki Senzaki

Received: 14 June 2013 / Accepted: 27 September 2013 / Published online: 13 October 2013

Abstract This study was undertaken to test the hypothesis that noninvasive echocardiographic indexes obtained using early diastolic mitral annular and inflow velocities reflect diastolic function in children. We included in this study 61 consecutive pediatric patients (age 0.4–13 years) who underwent cardiac catheterization for various heart diseases with biventricular circulation. Left ventricular (LV) pressure was measured using a high-fidelity manometer to obtain the time constant of relaxation (τ) and LV chamber stiffness (K). Echocardiography was simultaneously performed during catheterization. Data acquisition was repeated after the administration of dobutamine. The peak early mitral annular velocity (e') and τ showed a significant inverse correlation ($r = -0.42$). Receiver-operating characteristic (ROC) analysis to determine the 90th percentile of τ yielded an area under the curve (AUC) of 0.86 for a septal $e' < 6.2$ cm/s, with sensitivity and specificity of 0.83. The dobutamine-induced changes in e' closely correlated with those in τ ($r = -0.69$). The deceleration time (DT) showed a significant but weak negative correlation with K ($r = -0.35$), and ROC analysis to determine the 90th percentile of K yielded an AUC of 0.82 for a DT <100 ms, with sensitivity of 0.80 and specificity of 0.77. The ratio of peak early mitral inflow velocity (E) to e' (E/e') significantly correlated with LV end-diastolic pressure (EDP; $r = 0.48$, $P < 0.0005$), and ROC analysis to determine the 90th percentile of EDP (>12.96 mmHg) yielded an AUC of 0.81 for an $E/e' > 16.4$, with sensitivity of 0.71 and specificity of 0.93. The e', DT, and E/e' values in our study reflect the diastolic function in our pediatric population. However, the weak correlations between these indexes and invasive measures of diastolic function suggest that these indexes are useful in detecting diastolic dysfunction but not in determining the absolute values of diastolic dysfunction. Therefore, a future study is warranted to develop an efficient algorithm for systematic noninvasive evaluation of LV diastolic function in children.

Keywords Diastolic function · Stiffness · Relaxation · Tissue Doppler · Echo

S. Masutani · H. Saiki · C. Kurishima · S. Kuwata · M. Tamura · H. Senzaki (✉)
Department of Pediatric Cardiology, Saitama Medical Center, Saitama Medical University, 1981 Kamoda, Kawagoe, Saitama 350-8550, Japan
e-mail: hsenzaki@saitama-med.ac.jp

Introduction

A growing body of evidence highlights the diagnostic and prognostic importance of left ventricular (LV) diastolic function. The rate of LV relaxation characterizes the early phase of diastolic function, whereas LV stiffness (or compliance) represents the subsequent phase of diastolic function following LV relaxation. The interaction of these two diastolic properties determines the LV end-diastolic pressure (EDP), a representative measure of overall diastolic function, which is directly linked with clinical signs and symptoms of heart failure. Therefore the assessment, particularly by noninvasive methods (e.g., echocardiography), of the rate of LV relaxation, LV stiffness, and LV EDP as key parameters of diastolic function is of great clinical importance. In this regard, the rate of LV relaxation can be noninvasively evaluated by measuring peak early mitral annular velocity (e'); LV chamber stiffness (K), by the deceleration time (DT) of peak early mitral inflow velocity (E); and EDP, by the ratio of E to e' (E/e')

[1–6]. These echocardiographic indexes have been shown to be useful and reliable for routine clinical evaluation of diastolic function in adults, and many clinical guidelines use these indexes to stratify the severity of diastolic dysfunction [7].

The same indexes have been widely used recently in clinical evaluations in children [8–11], based upon the assumption that echocardiographic diastolic indexes in children have a relationship with invasively obtained indexes similar to that in adults (e'-relaxation, DT-stiffness, and E/e'-filling pressure relationships). However, these measurements depend greatly on loading conditions and heart rates, which are quite different in children and adults. Therefore, validation studies to verify such assumptions are necessary to accurately interpret these findings in children. In addition, recent reports suggest that echocardiographic indexes have significant limitations when applied to specific conditions such as advanced heart failure and hypertrophic cardiomyopathy, even in adults [12, 13]. Thus far, no study has systematically tested whether these noninvasive measures of diastolic function can be applied to children, and the few studies that have attempted to assess the relationship between noninvasive measurements and invasive criterion standard indexes in children have reported conflicting results. Therefore, it remains unclear as to whether these noninvasive indexes accurately represent diastolic function in children. This study was undertaken to test the hypothesis that noninvasive echocardiographic diastolic indexes sufficiently indicate diastolic function in children with heart disease.

Patients and methods

Patients

This study included 61 pediatric patients (30 male and 31 female; age: mean ± standard deviation (SD), 3.0 ± 3.1 years; range, 0.4–13.2 years; median, 1.7 years) with biventricular circulation who had no apparent structural abnormality of the mitral valve. The patients underwent diagnostic or interventional cardiac catheterization at Saitama Medical University, with written informed parental consent obtained for all the patients. Dobutamine was used to assess adrenergic reserve function in a randomly selected subgroup of children, and the indication of the dobutamine stress test was based on the guidelines for the Clinical Application of Echocardiography [available at http://www.j-circ.or.jp/guideline/pdf/JCS2010yoshida.h.pdf (in Japanese), Japanese Circulation Society, 2010]. The Saitama Medical University Institutional Review Board approved this validation study of echo-derived indexes in comparison with catheter-based invasive indexes (no. 11-144).

Measurements

All measurements were obtained during routine cardiac catheterization before angiography/ventriculography. LV pressures were measured using a high-fidelity micromanometer mounted on a 0.014-inch guide wire (RADI Medical Systems, Uppsala, Sweden) placed within a 4-F pigtail catheter [14]. Pressure data were digitalized at 500 Hz and stored for subsequent offline analysis by a custom-designed data-acquisition system.

Ventricular systolic and diastolic functions were noninvasively assessed by transthoracic two-dimensional color and pulsed Doppler echocardiography, and pulsed tissue-Doppler echocardiography during cardiac catheterization using a 5-, 8-, or 12-MHz transducer on a commercially available unit (Philips SONOS 5500). The transmitral inflow pattern was measured at the tip of the mitral valve, and the peak velocities during early diastole (E, cm/s) and atrial contraction (A, cm/s), and E DT (ms) were determined. Peak early mitral annular velocity (e') was determined using tissue-Doppler imaging (TDI) of the septal mitral annulus obtained on the apical four-chamber view [10, 15, 16]. The internal LV diameters were measured on the parasternal long-axis view [17]. The LV volume was calculated using the Teichholz method [18].

To determine whether changes in e' can reflect changes in LV relaxation induced by β-adrenergic stimulation, we repeated the measurements in a subgroup of 17 patients after administration of a small dose of dobutamine (5 μg kg^{-1} min^{-1}) over 10 min.

Data analysis

Invasive diastolic indexes

Time constant of LV pressure decay, an index of LV relaxation, was calculated using the nonzero asymptote of monoexponential pressure decay [19] and logistic fit [20] (τ_{ME} and τ_L, respectively). LV EDP was defined as the relative minimal LV pressure following the A wave [21]. If the minimal LV pressure was not clearly apparent, LV EDP was defined as the pressure just before the onset of rapid increase in LV systolic pressure. LV EDP and minimum pressure (LVPmin) were identified during the expiratory phase, and the mean values of three beats were used. LV chamber stiffness (K) was calculated as follows:

$$K = (\text{LV EDP} - \text{LVP min})/(\text{LV EDV} - \text{LV ESV}) \times \text{BSA}\left(\text{mmHg/ml} \times \text{m}^2\right),$$

where EDV and ESV represent LV end-diastolic and end-systolic volume, respectively. K was calculated using the Teichholz method [18] and the Fick method.

Statistical analysis and validation of echocardiographic diastolic indexes

Data were expressed as mean ± SD. Correlations between noninvasive and invasive indexes of diastolic function were tested using the Pearson correlation coefficient. $P < 0.05$ was considered statistically significant. To further explore the clinical utility of noninvasive diastolic echocardiographic indexes for detecting impaired diastolic function, a receiver-operating characteristic (ROC) curve analysis was performed to test whether e', DT, and E/e' can be used to determine the 90th percentile of invasive diastolic indexes of τ, K, and EDP, respectively. We used the 90th percentile of invasive indexes for ROC curve analysis because the 90th percentile of the LV EDP of the study patients, i.e., 12.96 mmHg, approached the upper limit of the reference range of LV EDP [18]. All statistical analyses were performed using JMP version 8 (SAS Institute, Cary, NC, USA).

Results

Table 1 lists the cardiac diseases of the patients in our study. Fifty (82 %) of 61 patients had no evidence of left-to-right or right-to-left shunt. The pulmonary-to-systemic flow ratio (Q_p/Q_s) in the remaining 11 patients ranged from 0.7 to 2.3 (1.4 ± 0.5). The demographic and hemodynamic data of all 61 patients are summarized in Table 2. Figure 1 displays representative Doppler and TDI results showing E, e', and DT on echocardiography.

Inverse correlation between e' and the relaxation time constant

The relationship between LV relaxation rate and e' was investigated for noninvasive evaluation of LV relaxation. Figure 2 (upper panels) shows a significant inverse correlation between e' and the time constant of LV relaxation (τ_L: $r = -0.42$, $P < 0.0005$ and τ_{ME}: $r = -0.42$, $P < 0.0005$). ROC curve analysis revealed that septal $e' < 6.2$ had an area under the curve (AUC) of 0.86, with sensitivity and specificity of 0.83 to determine the 90th percentile of τ_L (>23.55). Septal $e' < 7.8$ had an AUC of 0.83 with sensitivity of 1.0 and specificity of 0.57 to determine the 90th percentile of τ_{ME} (>47.68; lower panels in Fig. 2). These results indicate the usefulness of e' in detecting abnormally slow LV relaxation in children. In addition, dobutamine-induced changes in e' were closely correlated

Table 1 Diagnoses in the disease group

Diagnosis (n = 61)	n
After radical operation (n = 44)	
Tetralogy of Fallot	15
Transposition of great arteries	9
Coarctation of the aorta	8
Ventricular septal defect	4
Aortic regurgitation	2
Double outlet right ventricle	2
Total anomalous pulmonary venous connection	2
Congenitally corrected transposition of great arteries	1
Pulmonary atresia (Brock operation)	1
After palliative operation (n = 7)	
Tetralogy of Fallot, shunt	4
Ventricular septal defect, pulmonary arterial banding	1
Ebstein anomaly, coarctectomy, and pulmonary arterial banding	1
Interruption of aortic arch complex, Damus–Kaye–Stansel operation	1
Not operated (n = 10)	
Aortic stenosis	3
Kawasaki disease	3
Patent ductus arteriosus	2
Peripheral pulmonary stenosis	1
Pulmonary stenosis	1

Table 2 Demographic and hemodynamic data of the study population

	Mean ± SD	Median	Range
Demographic			
Age (years)	3.0 ± 3.1	1.7	0.4–13.2
Body weight (kg)	12.4 ± 7.6	10.3	4.2–41.5
Body height (cm)	85.6 ± 21.1	80.5	57–152
Body surface area (m^2)	0.53 ± 0.23	0.47	0.25–1.34
Catheterization			
Q_p/Q_s	1.1 ± 0.25	1	0.72–2.3
Heart rate (beats/min)	110 ± 21	110	65–167
LV systolic pressure (mmHg)	90 ± 18	89	57–152
LV EDP (mmHg)	9.2 ± 3.2	9.0	4.5–19.4
LV dP/dTmax (mmHg/s)	1246 ± 397	1234	478–2676
Echocardiography			
E (cm/s)	90 ± 24	91	31–140
A (cm/s) (n = 46)	63 ± 23	60	22–143
E/A (n = 46)	1.5 ± 0.65	1.4	0.58–4.4
Ejection fraction (%)	66 ± 10	68	44–89
Hormone			
BNP (pg/ml)	48 ± 73	27	4–518

Q_p/Q_s, Pulmonary-to-systemic flow ratio, *LV* left ventricular, *dP/dTmax* maximal rate of rise of pressure, *EDP* end-diastolic pressure, *E* early mitral inflow velocity, *A* late mitral inflow velocity, *BNP* plasma brain natriuretic peptide level

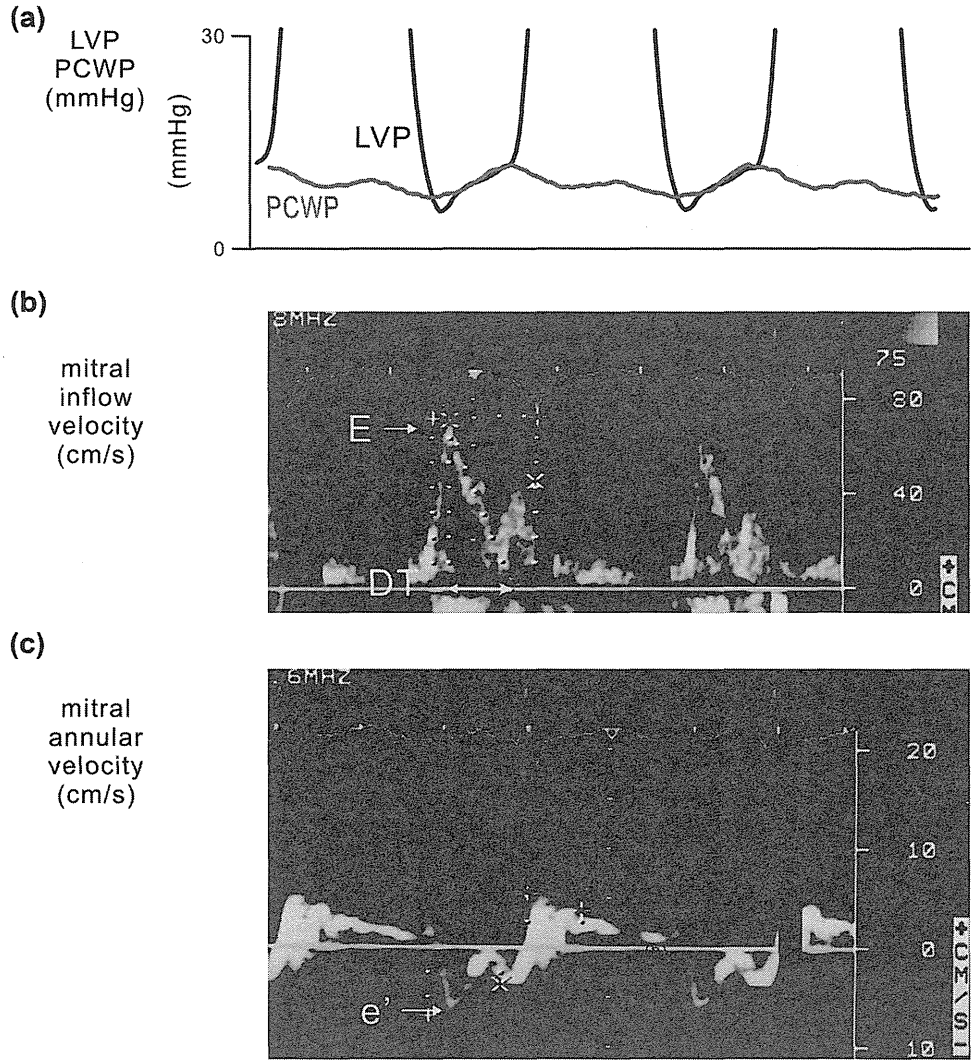

Fig. 1 Representative Doppler and tissue-Doppler images showing the peak mitral inflow velocity during early diastole (*E*), peak mitral annular velocity during early diastole (*e'*), and deceleration time (DT) of early mitral inflow velocity on echocardiography. **a** Left ventricular pressure (LVP; *black line*) and pulmonary capillary wedge pressure (PCWP; *purple line*). PCWP was time shifted to match the PCWP and LVP at the end of long-term diastasis. **b** Mitral inflow velocity by pulse-wave Doppler echocardiography. **c** Tissue-Doppler images of septal mitral annulus

with those in τ_{ME} and τ_L (τ_{ME}: $r = -0.69$, $P < 0.005$ and τ_L: $r = -0.59$, $P < 0.05$; Fig. 3).

Weak inverse correlation between DT and chamber stiffness

The relationship between K and DT was investigated for noninvasive evaluation of LV stiffness. K, calculated from echo-derived stroke volume and Fick-derived stroke volume, showed a weak but significant correlation with DT ($r = -0.30$, $P < 0.05$ and $r = -0.32$, $P < 0.05$, respectively; upper panels in Fig. 4). ROC curve analysis to determine the 90th percentile of K using the Teichholz method (>2.07 mmHg/ml × m^2) revealed that a DT <100 ms had an AUC of 0.82, with sensitivity of 0.80 and specificity of 0.77, and ROC curve analysis to determine the 90th percentile of K using the Fick method (>1.96 mmHg/ml × m^2) revealed that a DT <119 ms had an AUC of 0.70, with sensitivity of 1.0 and specificity of 0.49 (Fig. 4, lower panels). In summary, the relation between K and DT was significant but weak, and the ability of DT to detect LV stiffness was modest.

E/e' reflects LV EDP

The relationship between EDP and E/e' or DT was investigated for noninvasive evaluation of LV EDP. As shown in Fig. 5a and b, E/e' ($r = 0.48$, $P < 0.0005$) showed better correlation with LV EDP than DT ($r = 0.42$, $P < 0.005$). As shown in Fig. 5c, ROC curve analysis to determine the 90th percentile of LV EDP (12.96 mmHg) yielded an AUC of 0.81 by $E/e' > 16.4$, with sensitivity of 0.71 and specificity of 0.93. E/e' was superior to DT (AUC, 0.70). When the two parameters were combined by multivariable regression to estimate EDP, the estimation of EDP was much improved (estimated EDP = 9.3 + 0.38 × E/e' − 0.034 × DT; $r = 0.66$, $P < 0.0001$; Fig. 5d). Thus, a high E/e' ratio may predict a high LV EDP with high specificity, and the combination of E/e' and DT better predicts EDP than E/e' or DT alone.

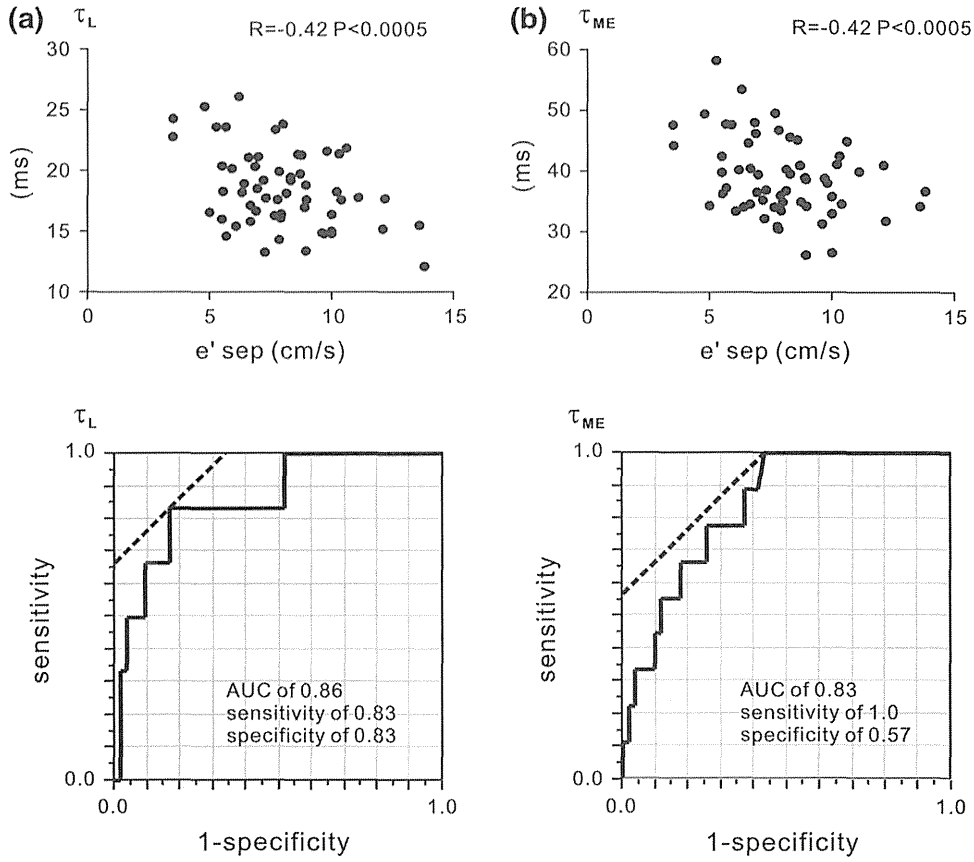

Fig. 2 Correlation between e' and the time constant of relaxation (τ_{ME} and τ_L). **a**, **b** Significant correlation was observed between e' and τ (τ_{ME}: $r = -0.42$, $P < 0.0005$ and τ_L: $r = -0.42$, $P < 0.0005$). Lower panes show the results of ROC curve analysis to determine the 90th percentile of τ_L and τ_{ME} by e', showing the ability of e' to detect abnormally slow relaxation

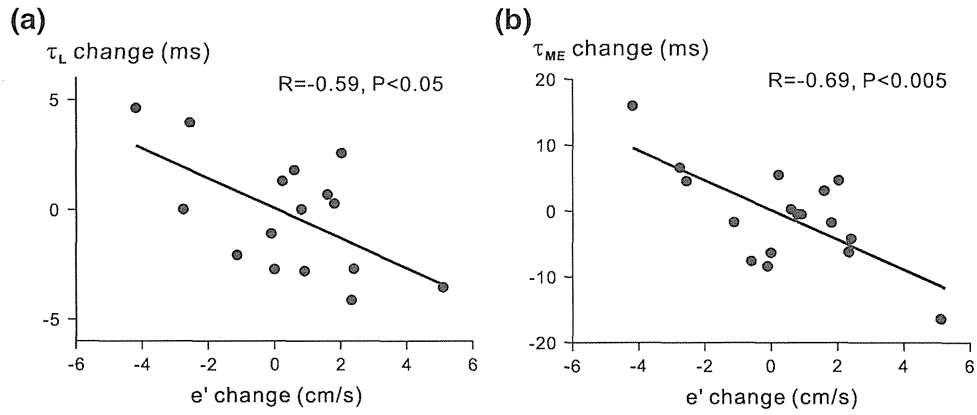

Fig. 3 Correlation between the dobutamine-induced changes in e' and the time constant of relaxation. Close correlation was observed between the dobutamine-induced changes in e' and the time constant of relaxation (τ_L: $r = -0.59$, $P < 0.05$ and τ_{ME}: $r = -0.69$, $P < 0.005$)

Discussion

The present study demonstrates that the correlations between e' and LV relaxation, DT, and stiffness, and E/e' and filling pressure were significant but not so strong in children with various heart diseases. However, the e', DT, and E/e' values in our study successfully detected impaired diastolic function (90th percentile of τ, K, and LV EDP, respectively), with acceptable AUC values. The improvement in the estimation of EDP by using both E/e' and DT indicates that combining multiple indexes may overcome the weakness of rough correlations and may improve the accuracy of diastolic assessment. Future large-scale studies are warranted to refine the cutoff values and to develop a definitive methodology and algorithm for systematic assessment of diastolic function in children.

Relaxation

Abnormality in LV relaxation is likely to precede an increase in LV stiffness, and LV relaxation becomes slower as diastolic dysfunction progresses. To the best of our knowledge, the e'-relaxation relationship in children was only reported in a study by Border et al. [22], who demonstrated that e' significantly correlated ($r = 0.58$, $P = 0.01$)

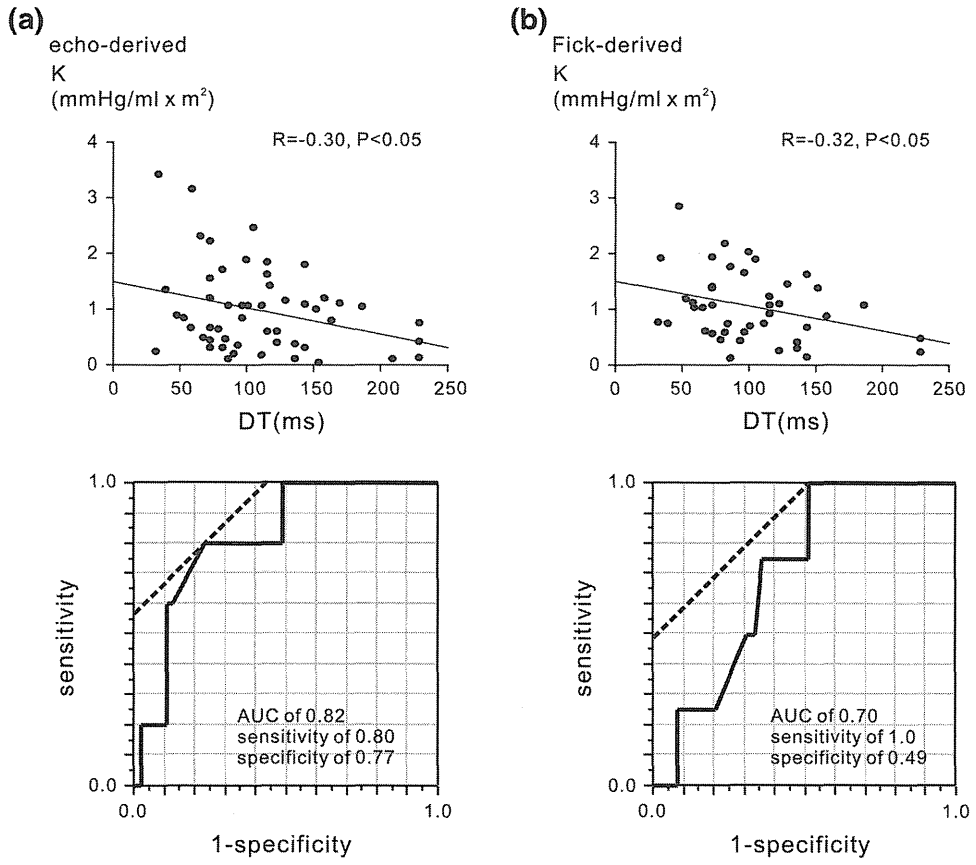

Fig. 4 Relationship between left ventricular chamber stiffness (K), calculated using **a** the Teichholz method (*closed circles*; $r = -0.28$, $P < 0.05$) and **b** the Fick method (*open triangles*; $r = -0.35$, $P < 0.05$), and deceleration time (DT), showing a weak inverse correlation between K and DT. The lower panel shows the results of ROC curve analysis to determine the 90th percentile of each K by DT

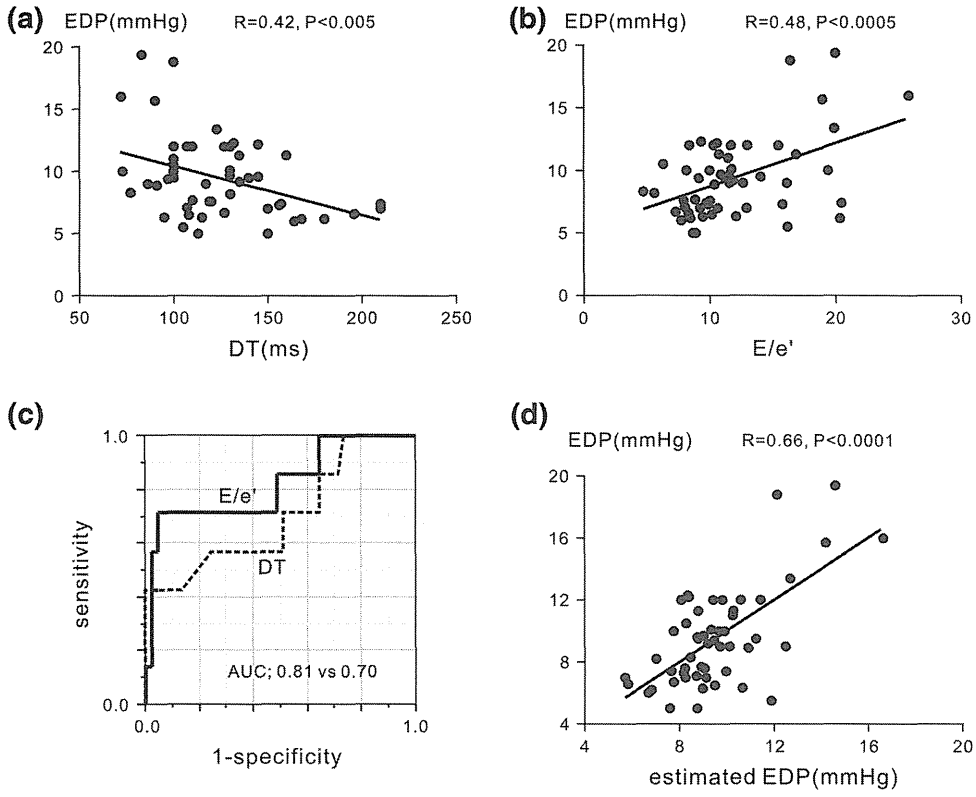

Fig. 5 Relationship between LV EDP, and E/e' and DT. **a** Relationship between LV EDP and DT ($r = 0.42$, $P < 0.005$), **b** relationship between LV EDP and E/e' ($r = 0.48$, $P < 0.0005$), and **c** results of ROC curve analysis to determine the 90th percentile of LV EDP by E/e' and DT. The E/e' shows a better ability to detect elevated LV EDP. **d** Relationship between LV EDP and estimated LV EDP by the combined model (estimated EDP = 9.3 + 0.38 × E/e' − 0.034 × DT; $r = 0.66$, $P < 0.0001$)